Hexaquarks at CLAS12

M.Bashkanov, G. Clash, M. Nicol, D.P. Watts, N. Zachariou

December 2019

Abstract

Recently discovered $d^*(2380)$ hexaquark is expected to be the first particle from a SU(3) hexaquark antidecuplet. A search for heavy strange partners of the $d^*(2380)$ is a challenging task. In this analysis note we propose strategies we plan to exploit in our studies of hexaquark antidecuplet. Most promising hexaquark candidates with strangeness zero, one, two, and three are identified and will be studied based on CLAS12 run group B data by the York group. Several PhD students are allocated for these studies.

1 Introduction

Quantum Chromo Dynamics (QCD) is responsible for the binding of quarks into hadrons. In resent years plenty new states in four-, five-, and six-quark sectors were discovered [1, 2, 3, 4, 5]. Some of them were properly identified as loosely bound molecular states. For many others the internal structure is not known, which raises a question of many-body effects in QCD, as well as the interplay between genuine multiquarks and molecular states. To properly study the internal structure of a composite state, large production rates together with ability of clean selection is required. This essentially rules out the detailed study of states with heavy quarks, since these cannot be produced in large quantities at the current experimental facilities. From another hand, four-and five-quark states made of only light quarks cannot be reliably disentangled from conventional states. That makes 6q states as a natural choice to study multiquark systems in vitro. Out of several 6q states we know, the $d^*(2380)$ with $J^P = 3^+$ is the most promising candidate: it is located far from any thresholds, and hence the 6q component - as opposed to the molecular one - is expected to be very large [3, 4, 5, 6, 7, 8, 9, 10, 11]. Theory studies also predict large hexaquark component for this state [12, 13]. Several opportunities are accessible for us in attacking multiquarks structure of 6q states.

1.1 Astrophysical implications of Hexaquarks

The role of a $d^*(2380)$ degree of freedom for the nuclear equation of state, EoS ([14]) was recently studied in several papers [15, 16]. The $d^*(2380)$ is a massive positively charged non-strange particle with integer spin (J=3) and it is the first predicted non-trivial hexaquark supported by experiment ([4, 5, 6]). The importance of such a new degree of freedom resides in the fact that it has the same u, d quark composition as neutrons and protons and, therefore, does not involve any strangeness degrees of freedom. Moreover, it is a boson and as such, has the possibility to condense within neutron stars. It was shown that despite its large mass, the $d^*(2380)$ can appear in the neutron star (NS) interior at densities similar to those predicted for the appearance of other proposed states e.g. nucleon resonances, Δ's, or hyperons. The effect of the $d^*(2380)$ on the nuclear equation of state (EoS) was studied both in non-interacting and interacting cases (both attractive and repulsive). The results indicate the $d^*(2380)$ has the potential to be an important new degree of freedom in neutron stars. Fractions of $d^*(2380)$ of around 20% are predicted in the centre of heavy stars, resulting in an increased maximum star radius and a reduced central density. New neutrino and antineutrino cooling mechanisms are possible with $d^*(2380)$ formation, which have previously not been included in neutron star modelling. The EoS with explicit $d^*(2380)$ degrees of freedom is one of the few which predict NS mass-radius relation consistent with the latest (subsequent) gravitational wave experimental results [17]. Indeed, the presence of the $d^*(2380)$ is predicted to set a strict limit on a maximum neutron star mass in agreement with that inferred from gravitational wave data [15, 16]. As an isoscalar particle the interaction of the d^* is reduced to isoscalar (dominantly σ, ω) exchanges. Interplay between the $d^*(2380)$ dimensionless coupling constants ($x_{\sigma d^*} = \frac{g_{\sigma d^*}}{g}$, $x_{\omega d^*} = \frac{g_{\omega d^*}}{g_{\omega N}}$) and its chemical potential in neutron star matter are shown on Fig. 1. As expected, an attractive interaction between the d^*'s and the nuclear matter leads to earlier appearance

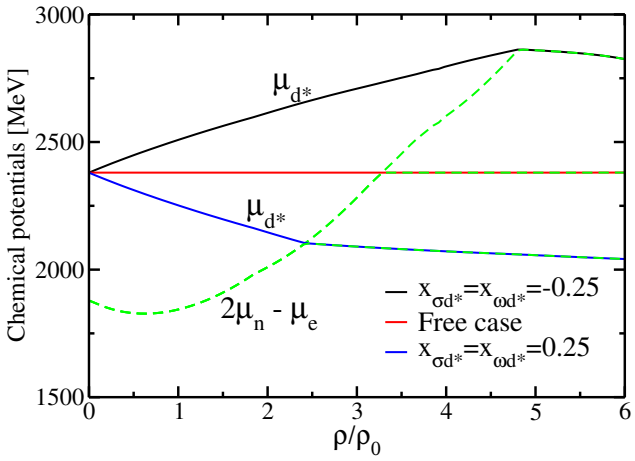

Figure 1: Chemical equilibrium condition for the appearance of the $d^*(2380)$ hexaquark in β-stable matter. Results are shown for the cases in which the $d^*(2380)$ feels attraction ($x_{\sigma d^*} = x_{\omega d^*} = 0.25$), repulsion ($x_{\sigma d^*} = x_{\omega d^*} = -0.25$) or does not interact at all with the rest of the particles of the system.

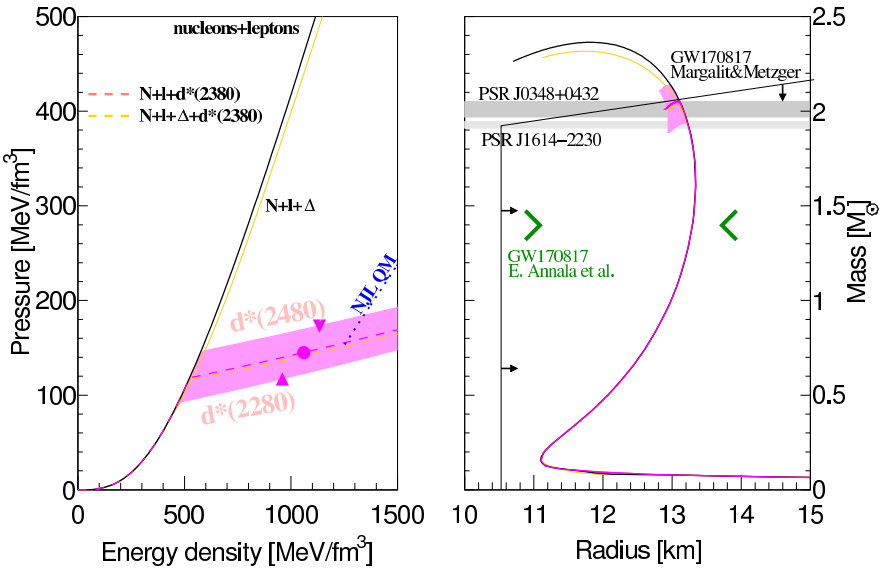

Figure 2: Neutron star EoS (left) and mass-radius relation (right) with and without the d^* degree of freedom. The predictions assuming $m_{d^*} = [2280, 2480]$ MeV and $m_{d^*} \equiv 2380$ MeV are shown by the shaded bands and dashed pink lines respectively. The effect of the Δ degree of freedom is shown as a gold line with $d^*(2380)$(dashed) and without (solid). The observational masses of the pulsars PSR J1614-2230 ($1.928 \pm 0.017 M_\odot$) [18] and PSR J0340+0432 ($2.01 \pm 0.04 M_\odot$) [19] as well as neutron star merger GW170817 limits from [17] and [20] are also shown. The pink markers on a left panel represent the maximum achievable pressure/energy density for heavy neutron star with d^* degrees of freedom for the $m_{d^*} = 2380$ MeV(circle), 2280 MeV and 2480 MeV(triangles). Pure NJL quark matter EoS is shown by dashed blue line.

of the d^* (in terms of nuclear density) in nuclear matter and a stronger reduction of the fractional protons and neutron composition [16]. The EoS and corresponding NS mass-radius relation in presence of the d^* can be seen on Fig. 2.

Furthermore, it was recently indicated that the Bose-Einstein condensates of the d^*-hexaquarks could be produced copiously in early universe and might contribute to dark matter, Fig. 3, see Ref. [21] for

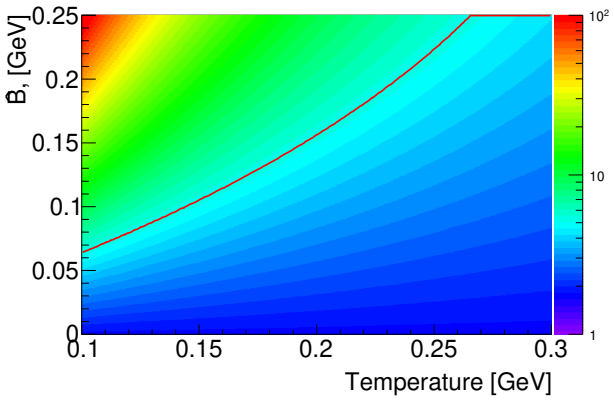

Figure 3: The primordial production of $d^*(2380)$-BEC (expressed as a ratio to baryon matter) calculated as a function of binding energy per baryon, $\hat{B}$ and matter-dark matter decoupling temperature. The red line shows the loci corresponding to the current experimental determination of the dark matter to matter ratio[**?**].

details. From these, it is clear that the extraction of the d^* properties, such as its size, structure, magnetic moment, quadrupole deformation have strong potential impact for astrophysics as well as for hadron and strong interaction physics. The properties of heavy d^* SU(3) multiplet members constrain the d^* structure (molecular vs hexaquark) as well as contribute to a "hyperon puzzle" problem and cooling of early Universe.

2 $d^*(2380)$ multiplet

As any strongly interacting particle, the $d^*(2380)$ appear as SU(3) multiplet member. Specifically, in the case of the $d^*(2380)$ it would be antidecuplet, Fig. 4. Spectroscopic study of other multiplet members can shed light on the d^* internal structure, complimentary to Form-Factor studies. In the molecular picture, the d^* SU(3) multiplet appear as a molecule made of two baryon decuplet members: from $\Delta\Delta$ for the $d^*(2380)$ to $\Delta\Omega$ for the d_{sss}, bound by a long-range pion exchange. However, since pion does not couple to strange quarks, the binding energy in molecules should decrease with increase of strangeness content. In a hexaquark picture the increase of mass driven by heavier s-quarks would imply stronger binding for the strange members. That is why we propose this measurement that will allow the discovery of all d^* multiplet members. This study will allow us to constrain 6q dynamics of multiquark systems.

Generally all d^*-multiplet members can decay into two baryon decuplet state or two baryon-octet states. The $d^*(2380)$ decays predominantly into two decuplet baryons – $\Delta\Delta$. Despite the fact that two octet baryons have much larger phase space, the decay brunch $Br(d^* \to pn) \sim 10\%$. The same is expected for all multiplet members, hence all decays would have large multiplicity final states.

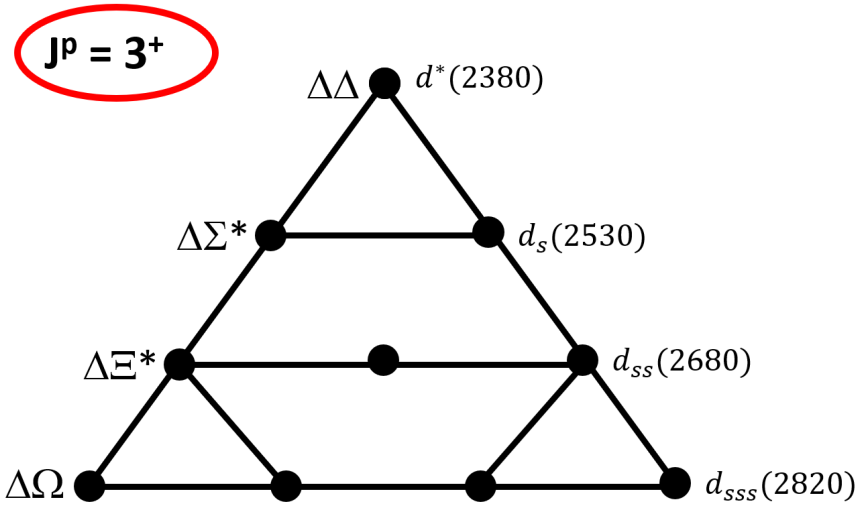

Figure 4: $d^*(2380)$ multiplet

3 $d^*(2380)$ photo and electroprduction.

The d^* electroproduction is an ultimate method to extract internal properties of the d^*. Similar studies were recently performed with various N^* resonances, where the measurement of transition form factor allowed to understand their nature (e.g. prove the molecular properties of the Ropper resonance, $N^*(1440)$). In the vast majority of electroproduction reactions, single photon exchange is the dominant process and two-photon exchange processes can be completely neglected. Unfortunately, this is not the case for the $d^*(2380)$, where the $d^* \to d\gamma\gamma$ transition is larger than $d^* \to d\gamma$. The majority - about 90% -of the d^* decay branches proceed via $d^* \to \Delta\Delta$ [11], in particular $Br(d^* \to \Delta\Delta \to d\pi\pi) \sim 37\%$. The photon decay of a Δ resonance is also large $Br(\Delta \to N\gamma) \sim 0.6\%$ or 0.7 MeV. Assuming these branching fractions and a total width of the $\Gamma(d^*) \approx 80$ MeV, one can estimate $\Gamma(d^* \to d\gamma\gamma) \approx 1.2$ keV. Similarly, one can evaluate the $\Gamma(d^* \to d\gamma)$ from A2 and ELPH measurements of the d^* photoproduction cross-section $\sigma(\gamma d \to d^* \to d\pi^0\pi^0) = 28nb$ [22, 23]. Accounting for a $Br(d^* \to d\pi^0\pi^0) = 14\%$, one will get $\sigma(\gamma d \to d^*) \sim 200\ nb$ or $\Gamma(d^* \to d\gamma) \sim 0.6\ keV$. Such unusually large ratio between double and single photon brunches might lead to a strong interference effects in d^*-electroproduction making experiment more sensitive to exotic degrees of freedom. However, it also requires better knowledge of the single photon brunch. Fortunately, such studies can be performed with an independent experiment with a real photon beam.

3.1 d^* photoproduction

With deuteron quantum numbers of $J^p = 1^+$ and the d^* being $J^p = 3^+$ there are only three possible multipolarities which can be involved in $\gamma d \to d^*$: $E2, M3$ and $E4$. On a quark level, that would correspond to a spin-flip of a 2,3 and 4 quarks respectively [1]. These transitions are proportional to the electric transition quadrupole moment, $Q_{d\to d^*}$, to the magnetic transition octupole moment, $\Omega_{d\to d^*}$, and to the electric transition hexadecupole moment $D_{d\to d^*}$, respectively [24]. The $E4$ transition is expected to be highly suppressed, and therefore we assume in all subsequent chapters that only $E2$ and $M3$ transitions contribute (unless otherwise explicitly stated). There are two and only two channels where the d^* can be observed in photo-/electro- production: $d^* \to d\pi^0\pi^0$ and $d^* \to pn$. In the later, a partial wave decomposition is essential. In any other channels, including $d^* \to d\pi^+\pi^-$ the level of conventional background exceeding the d^* signal by 2-3 orders of magnitude making any reliable analysis challenging. Both $d^* \to d\pi^0\pi^0$ and $d^* \to pn$ channels were analysed intensively with the Crystal Ball, at MAMI Mainz. Details can be found in Refs. [25, 26]. An exploratory analysis is foreseen for the $d^* \to d\pi^0\pi^0$ channel Fig.5, while deuteron electrodisintegration reaction is a standard calibration process for many run groups, so no further simulation studies are necessary.

It was recently shown [27] that one can access the NN^* Final State Interaction (FSI) in $\gamma d \to d\pi^0\pi^0$. While the data of Ref.[27] were not very conclusive, such a possibility requires an independent check.

As a starting point we have simulated Phase Space $ed \to e'd\pi^0\pi^0$ weighted with $1/q^2$ dependence for the virtual photon, Fig.5. The expected acceptance is fairly low, however in case of one or two π^0 detection, the energy dependence of acceptance is fairly smooth and rather flat which ensure the absence of acceptance related bump production. The expected statistics is rather low. We expect few thousands of reconstructed events up to 3rd resonance region. It should be sufficient for an exploratory analysis, to identify possible issues with this channel.

[1] Generally one would expect that higher multipoles should be suppressed and that the main transition amplitude should be $E2$. In a similar case of $N \to \Delta$ transition the main multipole is $M1$ with $E2$ being of a few percent only.

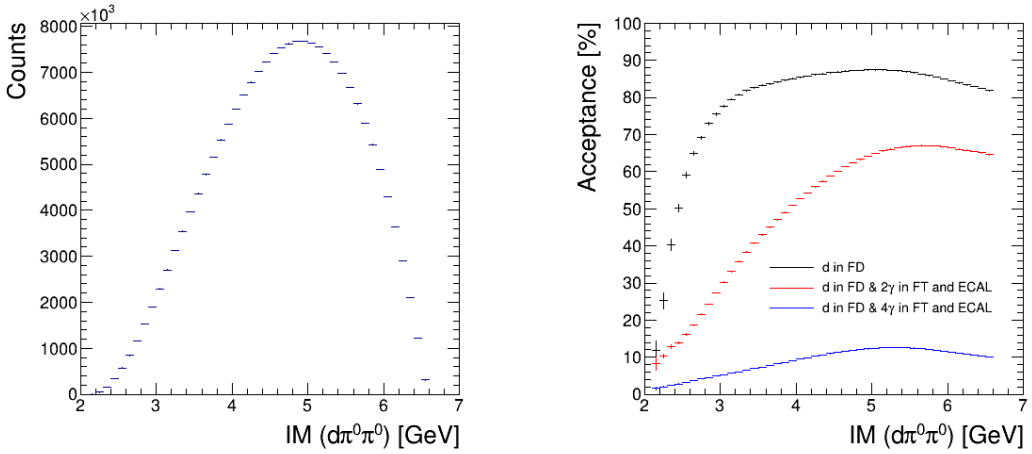

Figure 5: Simulated $d\pi^0\pi^0$ invariant mass(left) and reaction acceptance as a function of $M_{d\pi\pi}$ (right). Phase space MC with $1/q^2$ weight for a virtual photon. Black line correspond to acceptance of the reaction if only deuteron are measured in FD; red: d in FD and 2 photons in FT/ECAL; blue: d in FD, 4 photons in FT/ECAL

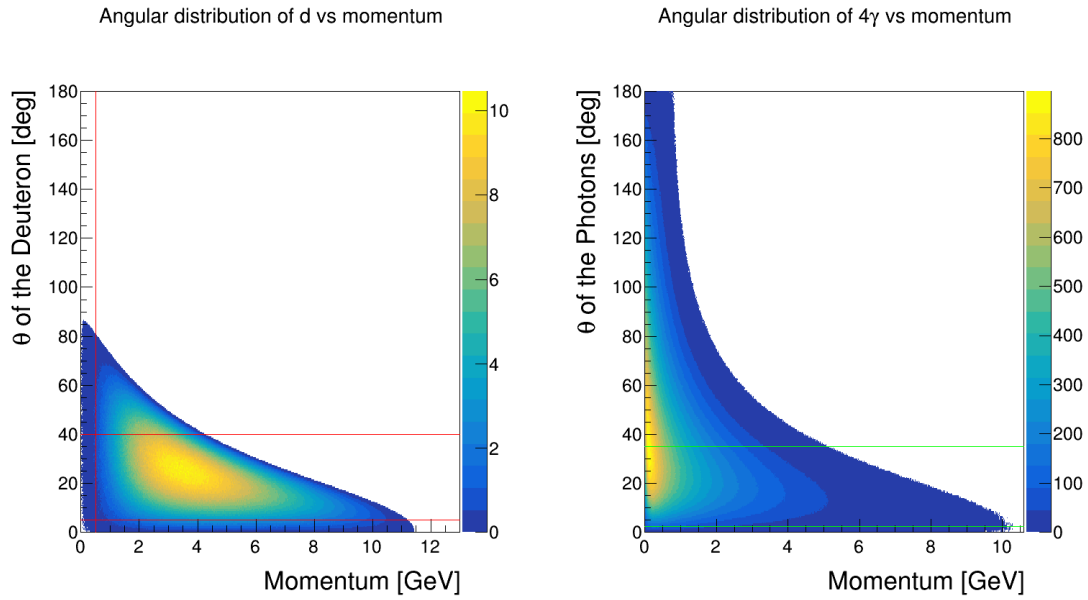

Figure 6: Simulated angular distributions for the $\gamma^* d \to d\pi^0\pi^0$ events

4 d_s -state

There was preliminary d_s search performed based on CLAS6 g13 data attempting to study $d_s \to \Sigma^*\Delta$ decay $d_s \to \Sigma^{*-}\Delta^{++} \to \Lambda\pi^- p\pi^+ \to 2\pi^- 2p\pi^+$. To conserve strangeness a d_s production needs to be accompanied by kaon. With two charge states of d_s^+ and d_s^0 it could be both K^+ and K^0, however, to suppress diagrams with kaon in flight production(Fig 19), contributing largely to a background reactions we concentrate on a process with neutral kaon in a final state: $\gamma d \to K^0 d_s$. A typical diagram leading to production of the d_s is shown on Fig. 7.

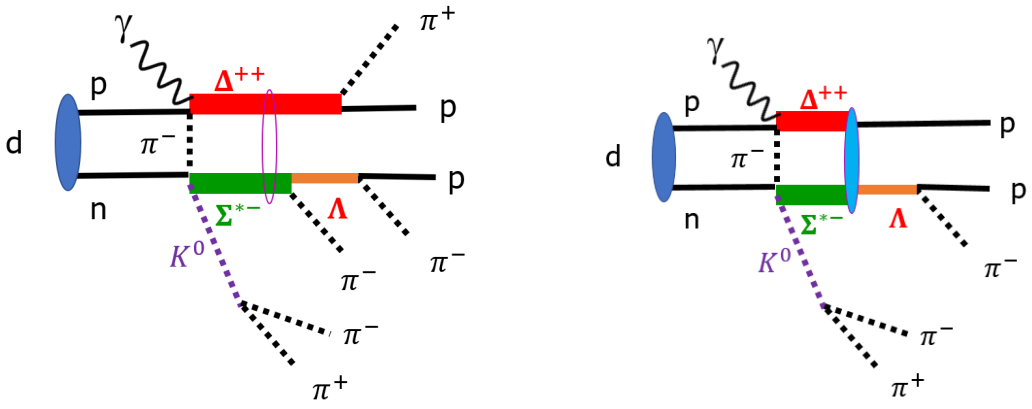

Figure 7: d_s photoproduction graph with decay to Decuplet+Decuplet (left) and Octet+Octet (right).

A very high-multiplicity final state for the reaction $\gamma d \to K^0 d_s \to 3\pi^- 2\pi^+ 2p$ reduce detection efficiency substantially, however as a byproduct it strongly increase the purity of selected process. Fig 8 show main steps of event selection. Resulting distribution shows pretty clean $\Sigma^*\Delta$ spectrum, which agrees very well

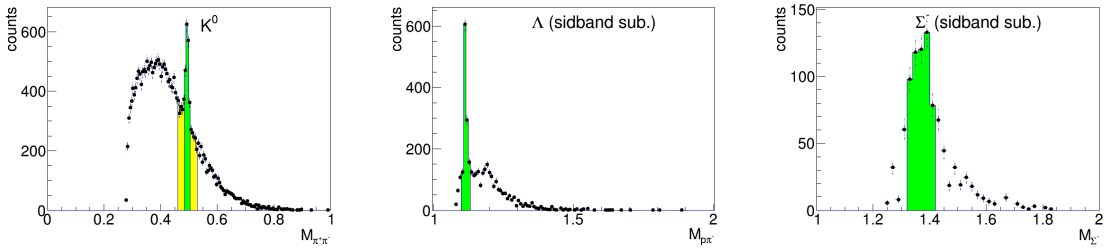

Figure 8: d_s selection steps. Left panel: K^0 selection from $\pi^+\pi^-$ signal(green) and side bands(yellow). Middle Panel: Λ selection from $p\pi^-$. Right Panel: Σ^* selection from $\Lambda\pi^-$

with simulations with possible but insignificant enhancement at d_s mass, Fig. 9.

Generally speaking, it should be sufficient to measure only the K^0, observing d_s in a missing mass spectrum. To increase statistics we consider to restrict ourselves to detection of K^0 to extract the missing mass and two protons to ensure two-nucleon dynamics of the reaction. This way also elastic channel $d_s \to \Lambda p$ can be partially accessed. We do not expect to see any signal in Λp channel, unless the polarisation observables based on Λ recoil polarisation are involved, similarly to $d^* \to p\vec{n}$ case. A detailed simulation studies of angular distributions and efficiencies can be seen in Fig 10 and Fig 11. The acceptance is smooth and rather large for such a many body final state.

We expect much larger d_s unrelated backgrounds in K^+ associated reactions. However, this does not exclude $\gamma^* d \to K^+ d_s^0$ from our shopping list especially in polarisation observables. Indeed, both decay branches $d_s^0 \to n\Lambda$ and $d_s^+ \to p\Lambda$ should lead to 100% polarisation of both nucleons and due to ${}^3D_3$ decay partial wave, but any single nucleon channel hyperon production does not need to have the same polarisation properties due to different photon-nucleon coupling for proton/neutron and due to difference in magnetic

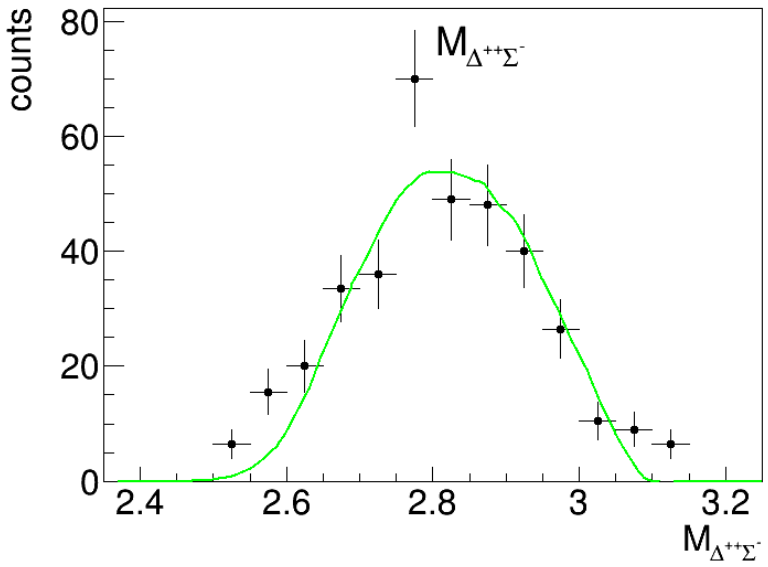

Figure 9: $\Sigma^*\Delta$ spectrum

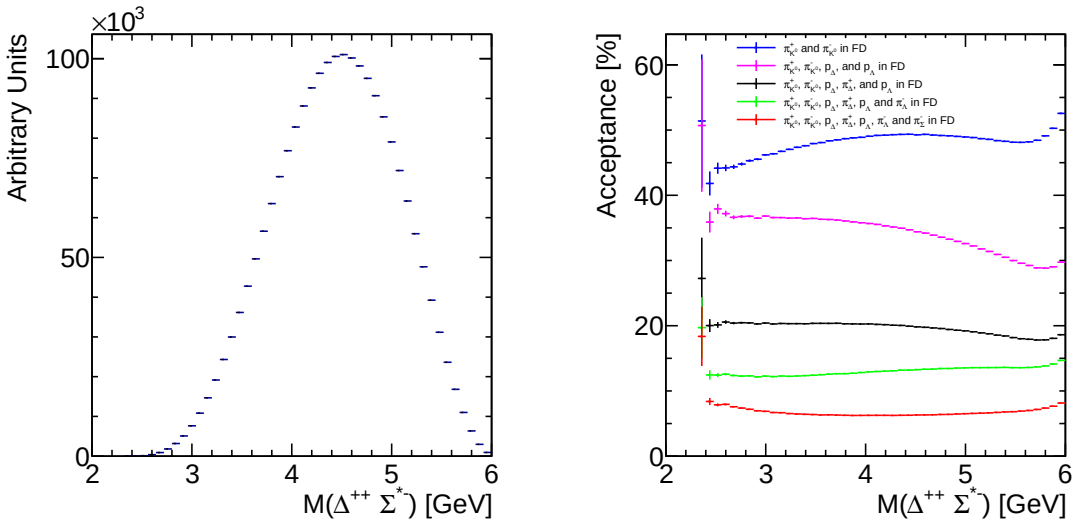

Figure 10: Simulated $\Delta\Sigma^*$ invariant mass(left) and reaction acceptance as a function of $M_{\Delta\Sigma^*}$ (right). (Phase Space MC with $1/q^2$ weight for a virtual photon.). Blue line correspond to acceptance of the reaction if only K^0 are measured in FD; pink: K^0 and 2 protons in FD; black: K^0, 2 proton and π^+ in FD; green: K^0, Δ and in FD; red: K^0, Δ and Σ in FD.

moments of protons/neutrons/N^*'s. That is why a comparison of $n\vec{\Lambda}$ and $p\vec{\Lambda}$ channels can be used for a better background understanding in these channels.

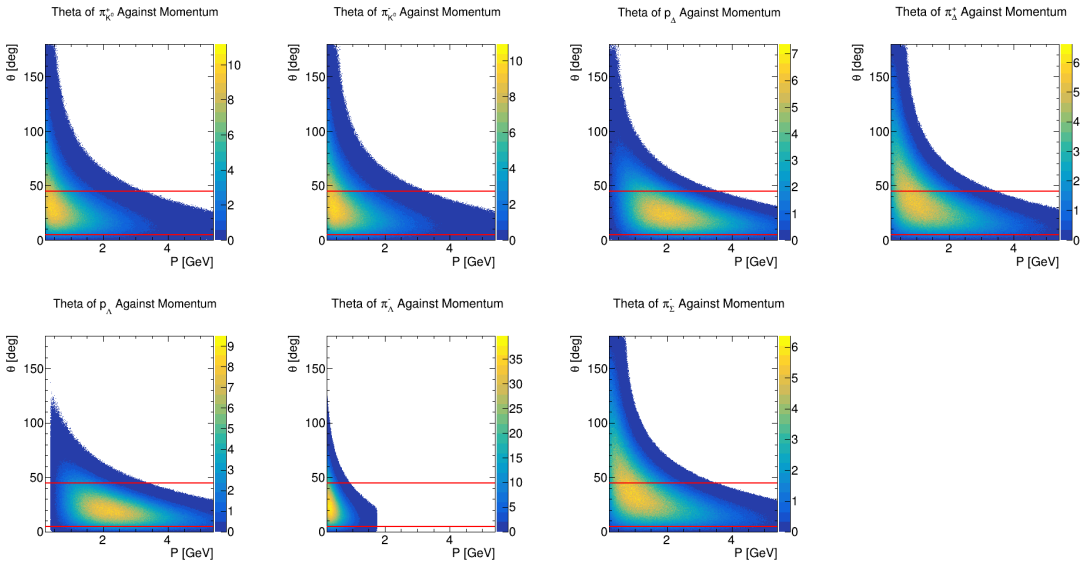

Figure 11: Simulated momentum-angular relations for the $\Delta\Sigma^*$ electroproduction reaction. Horizontal lines highlight the FD acceptance range.(Phase Space MC with $1/q^2$ weight for a virtual photon.)

5 d_{ss}-state

The d_{ss} state appears as an isotriplet with charges from -1 to +1. The most convenient state to search for appeared to be d_{ss}^{-}, since it is accompanied by two K^+ with fairly high detection efficiency and selection purity with positively charge outbending magnetic field. The main background processes originates from Ξ^{*-} production on proton and can be fairly well eliminated by comparison of $\gamma p \to K^+K^+X$ and $\gamma d \to K^+K^+X$ reactions. To increase purity of the sample and ensure the two-nucleon origin of the reaction we plan to require both protons to be detected as part of our selection criteria. The main physical background originates from

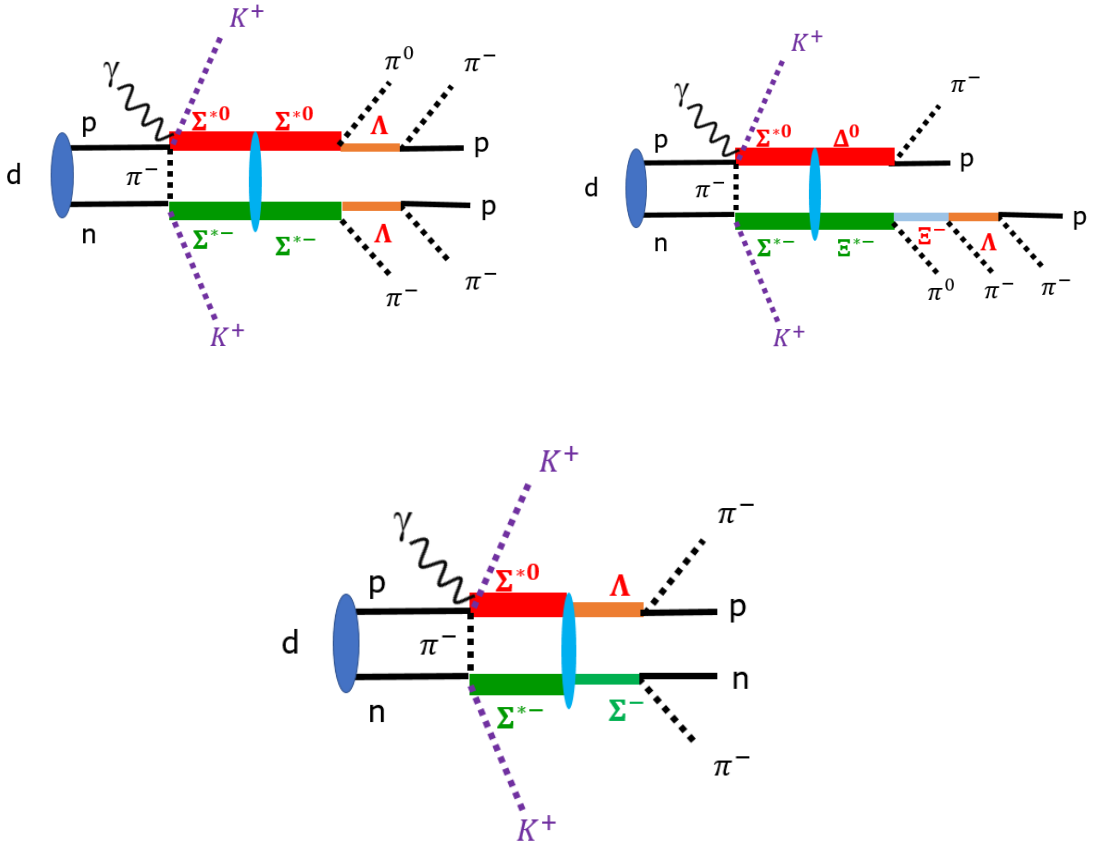

Figure 12: d_{ss} photoproduction graph with $10 \oplus 10$ decay(top row) and $8 \oplus 8$ decay (bottom).

Ξ^{*-} production on proton, however it worth noting that neither of known Ξ^{*-} states can build up a peak in the vicinity of d_{ss} mass, see Fig 13. Here we assumed the same suppression factor for the d_{ss} relative to conventional resonances as for the d^* relative to N^*/Δ's (~ 100 suppression). For simplicity, all known Ξ's are shown to appear with the same strength. As one can see the d_{ss} is expected to appear in the region where no Ξ contributes. If we assume a quasi-free K^+K^+ production on proton, Fig 13, the d_{ss} should appear at $M_{d_{ss}} - M_n$.

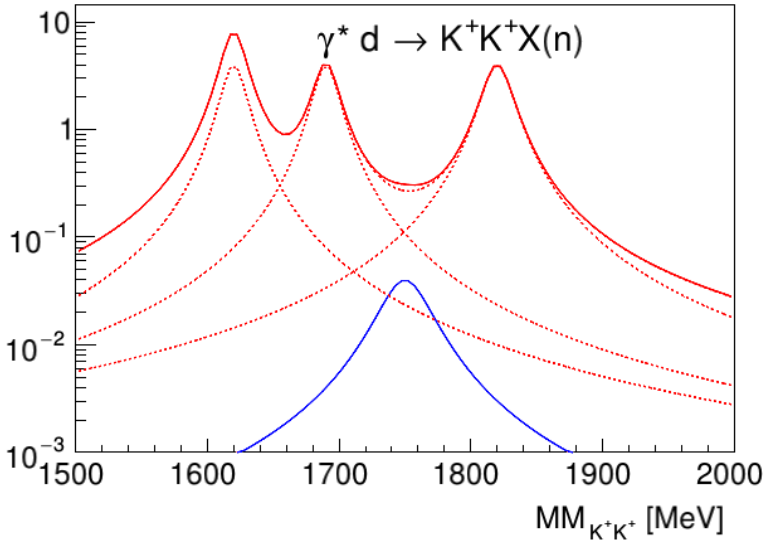

Figure 13: Conventional background in d_{ss} production for the reaction $\gamma d \to K^+K^+X$ without requirement on nucleons in the final state, under assumption of proton target (quasi-free process). Red lines correspond to known Ξ^* states, blue line represent d_{ss}.

6 d_{sss}-state

The d_{sss} state is an ultimate goal of the d^*-multiplet searches. It has isospin $I = 3/2$ and represented by 4 charge states from $q = -2$ to $q = +1$. The double negative member of isoquartet appeared to be a most promising one in terms of conventional background. Indeed, conventional background in a $\gamma p \to 3K^+X$ channel is strictly prohibited: to conserve both charge and strangeness the state X should have charge $q = -2$ and strangeness $s = -3$ which is impossible for a 3q state - the most negative and actually the only state with strangeness $s = -3$ is the Ω baryon has charge $q = -1$. For further discussion about possible nucleon based background for the d^{--}_{sss} see section 7. The reaction we are looking for in case of d^{--}_{sss} production can be seen of Fig. 14 A series of simulations were performed to understand the kinematics of

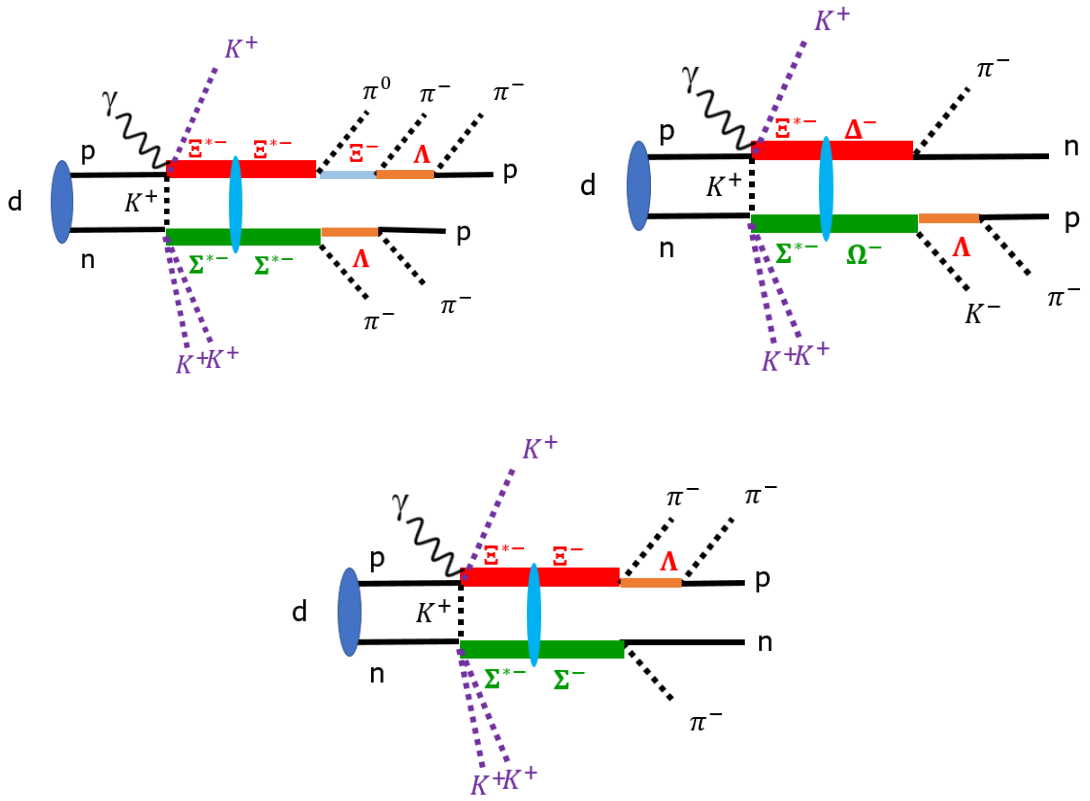

Figure 14: d^{--}_{sss} photoproduction graphs for the Decuplet-Decuplet decay (top row) and Octet-Octed decay bottom.

possible d^{--}_{sss} production.Its appeared to be that the angular distribution of all three K^+ is favourable to be detected with CLAS forward detector, the efficiency is very smooth: no sharp changes in efficiency is found, see Fig. 15. Several reaction decay brunches are possible to investigate here, both in $d_{sss} \to 10 \oplus 10$ and $d_{sss} \to 8 \oplus 8$ channels. There are two possible $d^{--}_{sss} \to 10 \oplus 10$ channels, $\Sigma^{*-}\Xi^{*-}$ with most promising decay chain $d^{--}_{sss} \to \Sigma^{*-}\Xi^{*-} \to (\Lambda\pi^-)(\Xi^0\pi^-) \to (p\pi^-)(\pi^-)(\Lambda\pi^0) \to 2p\pi^0 4\pi^-$ which has a branching ratio of 41%. The other $10 \oplus 10$ channel is $\Omega^-\Delta^-$ with most promising decay chain $d^{--}_{sss} \to \Omega^-\Delta^- \to (n\pi^-)(K^-\Lambda) \to npK^-2\pi^-$, which has branching ratio 44% .The only possible $d^{--}_{sss} \to 8 \oplus 8$ channel is $\Sigma^-\Xi^-$ with decay chain $d^{--}_{sss} \to \Sigma^-\Xi^- \to (n\pi^-)(\Lambda\pi^-) \to np3\pi^-(Br = 64\%)$, where full measurement of Λ provide access to a polarisation observables in d^{--}_{sss}.

As one can see in Fig. 15 the acceptance of the $d^{--}_{sss} \to \Omega^-\Delta^- \to (n\pi^-)(K^-\Lambda) \to npK^-2\pi^-$ reaction is very large even if all charged particles required to be measured in the FD. The acceptance is also very smooth, hence, no artificial bumps/deeps are expected to be produced by geometrical cuts.

In Fig. 16 one can see the angular distributions for the individual participants of the reaction $ed \to e'\Omega^-\Delta^- \to (n\pi^-)(K^-\Lambda) \to npK^-2\pi^-$, no d_{sss} formation condition was imposed. It is clear that the

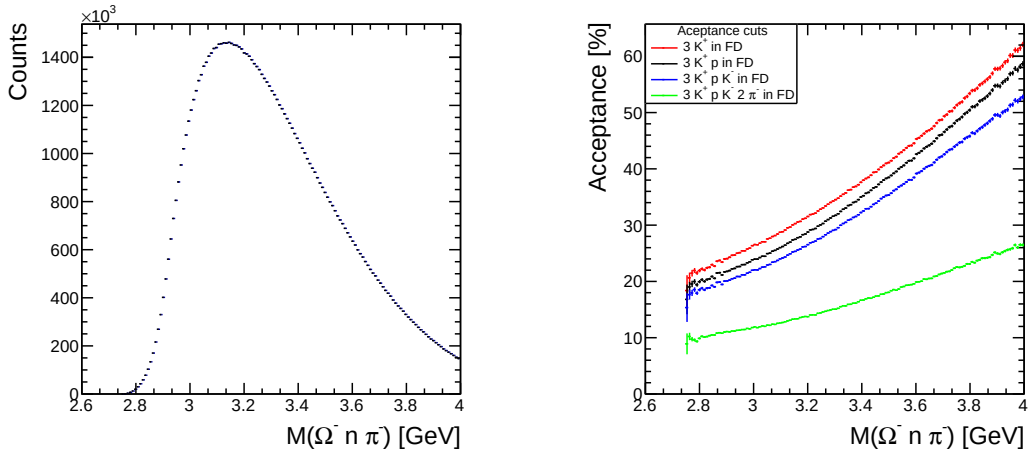

Figure 15: Simulated $\Omega\Delta$ invariant mass(left) and reaction acceptance as a function of $M_{\Omega\Delta}$ (right). Red line correspond to acceptance of the reaction if only $3K^+$ are measured in FD; black: $3K+$ and proton in FD; blue: $3K+$, proton and K^- in FD; green: $3K+$, proton, K^- and $2\pi^-$ in FD. (Phase space generation with $1/q^2$ weight for the virtual photon)

acceptance is large for all particles even if we limit ourselves for the FD detection only.

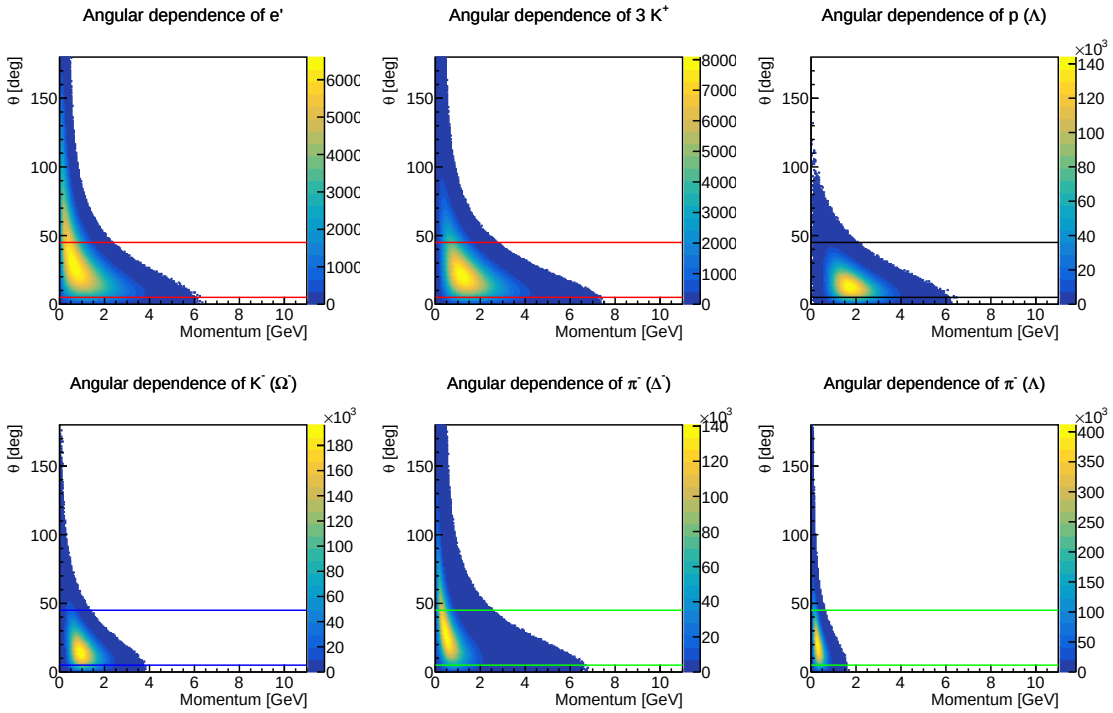

Figure 16: Simulated momentum-angular relations for the $\Omega\Delta$ electroproduction reaction. Horizontal lines highlight the FD acceptance range. (Phase space generation with $1/q^2$ weight for the virtual photon)

Since the fully exclusive reconstruction of the d_{sss} final state is challenging we also performed some studies on possibility of semi-inclusive analysis with $3K^+$ and a recoil electron being measured. The main

issue in this case would be a kaon misidentification. However, there are several reliable methods how it can be treated. The one, which we used for the benchmark studies of the rg-A data with single and double kaon production is a side-band subtraction of a kaon mass plot, Fig. 17.

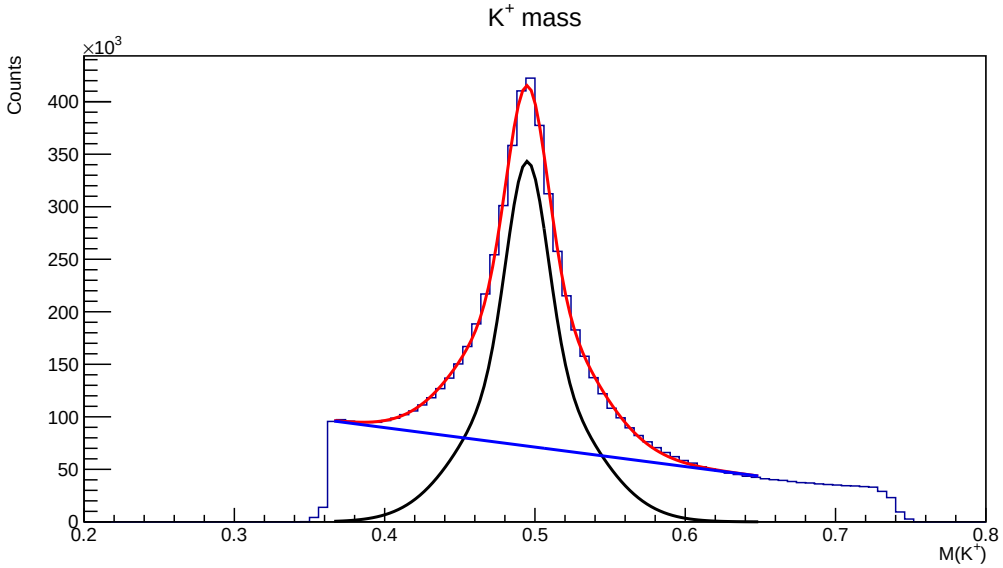

Figure 17: rg-A kaon mass plot distribution with particle mass calculated based on measured velocity (β) and particle momentum. Fitted curves showed peaked signal from kaon as well as a smooth misidentification background for the single K^+ production.

By defining signal and background side-bands as mean +/ 3 σ and mean +/- 6 σ to mean +/- 9 σ one can make a $e'K^+$ missing mass plot, Fig. 18.

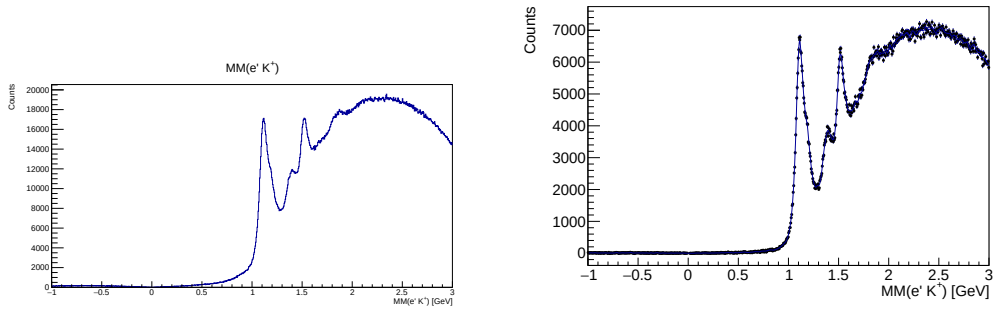

Figure 18: rg-A $e'K^+$ missing mass with (right) and without (left) side band subtraction based on kaon mass.(rg-A data)

As one can see, Fig. 18 the pion background, most vividly noticeable as a subthreshold surplus of events gets completely eliminated, Fig. 18(right). All hyperons are nicely visible. A broad bump under hyperon peaks do not originate from pion misidentification and/or event mixing. It comes form an in-flight kaon production, Fig. 19.

Similarly one can produce a side band subtracted $e'K^+K^+$ missing mass plot for a strangeness - 2 case, Fig. 20.

In this case one also can see the pion background completely eliminated and a first two cascades nicely visible on top of nearly no background. The main background has a physical origin as a kaon in-flight production, Fig. 19, and has very smooth behaviour.

These studies show clear potential for a $3K^+$ semi-inclusive analysis where comparison of a distributions from proton and deuteron targets can help to elucidate two-nucleon based $3K^+$ production processes.

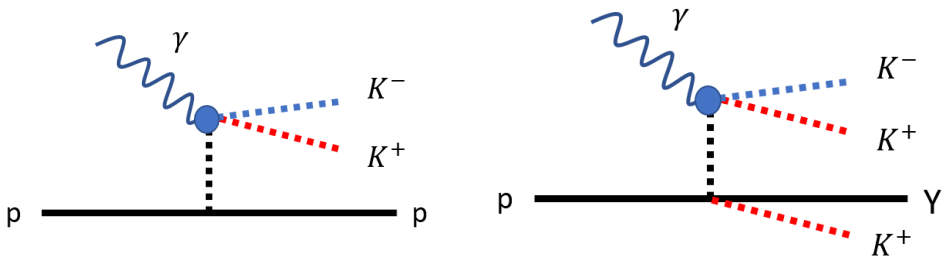

Figure 19: Diagrams of the typical kaon in-flight production background for single K^+ (left) and double-K^+ (right) production.

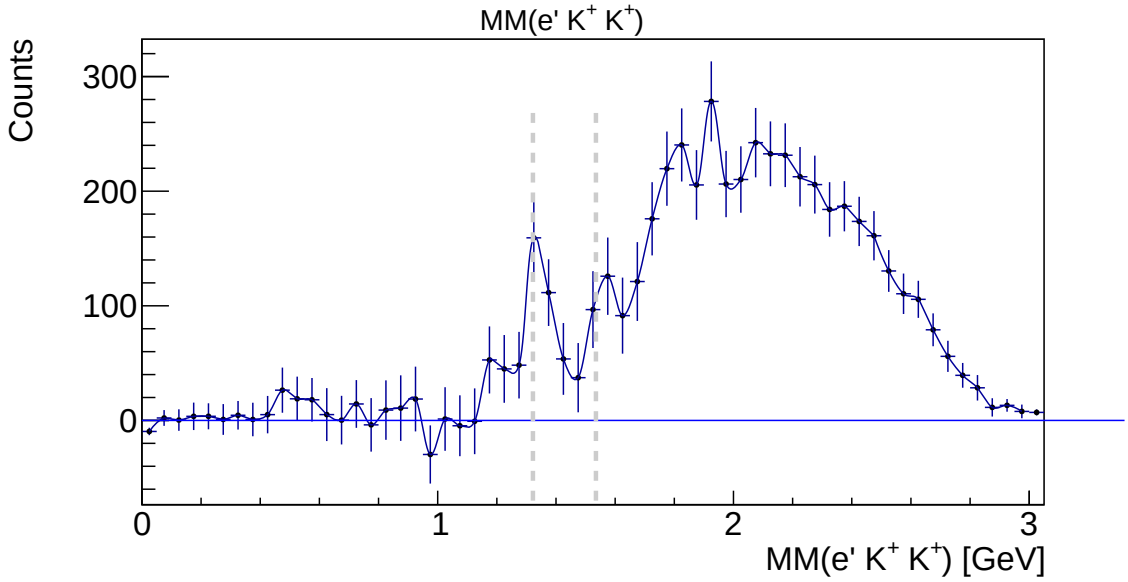

Figure 20: rg-A $e'K^+K^+$ missing mass with side band subtraction based on kaon mass.(rg-A data)

7 $\Omega\pi^-$ background for the d_{sss}-state

One should not expect any states in a strangeness $s = -3$ and charge $q = -2$ channel within simple quark model picture. The minimum configuration which can cover such quantum numbers is the $\Omega\pi^-$ channel. There were several recent studies related to Ω and Ω_c interactions with an octet of mesons [28, 29]. One can expect dynamically generated resonances in some channels but not in $\Omega\pi^-$. It was shown already in Ref. [28] that a $\Omega\pi$ contact term is very repulsive. Unfortunately, no coupled channel analysis of an $\Omega\pi$ system was performed so far, hence bumpy behaviour in an $\Omega\pi$ system due to coupled channels and/or threshold effects/cusp cannot be completely excluded.

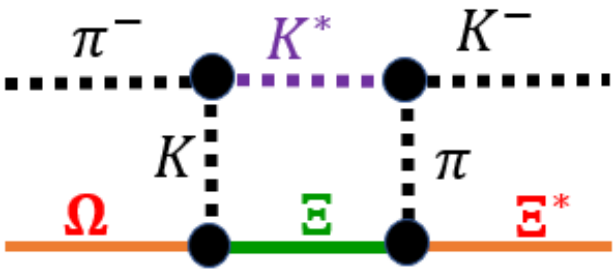

Figure 21: $\Omega\pi$ possible coupled channel graphs

One can identify three potentially dangerous regions near $\Omega\pi$, Ξ^*K and ΞK^* thresholds.

	$\Omega\pi$	Ξ^*K	ΞK^*
Threshold, MeV	1811	2024	2213
Width, MeV	0	10	51

It is interesting to note that the $\Omega\pi$ threshold lie even below the ΞK threshold (1815 MeV). We do not expect strong coupling between these two channels, however a closeness of two threshold 1811 MeV vs 1815 MeV might create some unusual behaviour. Study of this channel might provide important information about couple channel dynamics in exotic triply strange system as well as supply information about d_{sss} background.

First evaluation were preformed based on CLAS12 data rg-A data with electron in Forward Detector. All 3 positive Kaons were selected in FD with tight $\Delta\beta - p$ cuts tuned on exclusive $\gamma^* p \to K^+\Lambda$ reaction. The missing mass of e^-3K^+, without side band subtraction, shows very small count rate, Fig. 22, proving small background level for the d_{sss} production. Further increase in statistics might elucidate dynamics of an $\Omega\pi$ system. An absence of kaon mass side band subtraction is clearly visible since all the background is concentrated in kinematically forbidden subthreshold region.

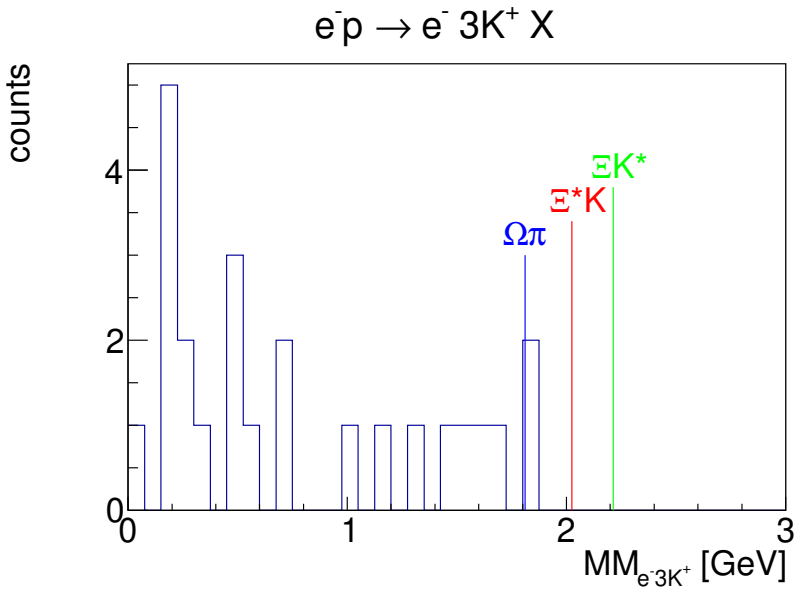

Figure 22: rg-A $\gamma^* p \to 3K^+X$ reaction study, $MM(e^-K^+K^+K^+)$. with appropriate thresholds shown as vertical lines.

References

[1] R. Aaij *et al.*, Phys. Rev. Lett. **112**, 222002, (2014)

[2] R. Aaij *et al.*, Phys. Rev. Lett. **122**, 222001, (2019)

[3] M. Bashkanov *et al.*, Phys. Rev. Lett. **102**, 052301 (2009).

[4] P. Adlarson *et al.*, Phys. Rev. Lett. **106**, 242302 (2011).

[5] P. Adlarson *et al.*, Phys. Rev. Lett. **112**, 202301 (2014).

[6] P. Adlarson *et al.*, Phys. Lett. B **721**, 229, (2013)

[7] P. Adlarson *et al.*, Phys. Rev. C **88**, 055208 (2013).

[8] P. Adlarson *et al.*, Phys. Lett. B **743**, 325 (2015).

[9] P. Adlarson *et al.*, Eur. Phys. J. A **52**, 147 (2016).

[10] P. Adlarson *et al.*, Phys. Rev. C **90**, 035204 (2014).

[11] M. Bashkanov, H. Clement, T. Skorodko, Eur. Phys. J. A **51** (2015) 7, 87.

[12] Fei Huang, Peng Nian Shen, Yu Bing Dong, Zong Ye Zhang, Sci. China Phys. Mech. Astron. **59**, 622002 (2016).

[13] M. Bashkanov, Stanley J. Brodsky, H. Clement Phys.Lett. B**727**, (2013), 438-442

[14] I. Vidaña Hyperon puzzle, Proceedings of the Royal Society A474, 20180145

[15] I. Vidaña, M. Bashkanov, D.P. Watts, A. Pastore, Phys. Lett. B **781**, 112-116, (2018).

[16] A. Mantziris, I. Vidaña, M. Bashkanov, D.P. Watts, A. Pastore, A.M. Romero, arXiv:2002.06571.

[17] Ben Margalit and Brian D. Metzger, Astrophys.J. 850, no.2, L19 (2017)

[18] P. Demorest, T. Pennucci, S. Ransom, M. Roberts, J. Hessels, Nature **467**, 1081 (2010).

[19] J. Antoniadis *e*t al., Science **340** 6131(2013).

[20] E.Annala *et al.*, arXiv:1711.02644v1

[21] M. Bashkanov and D.P. Watts, J. Phys G **47**, no.3, 03LT01, (2020)

[22] M. Guenther, Master Thesis, University of Basel (2015); PoS (Hadron2017) 051.

[23] T. Ishikawa *et al.*, Phys. Lett. B **772**, 398, (2017).

[24] M. Bashkanov and D.P. Watts, Phys. Rev. C **100**, no.1, 012201, (2019)

[25] M. Bashkanov *et al.*, Phys. Lett. B**789**, 7, (2019).

[26] M. Bashkanov *et al.*, , Phys. Rev. Lett. **124**, 132001, (2020)

[27] T. Ishikawa *et al.*, Phys. Lett. B **789**, 413, (2019).

[28] E.E. Kolomeitsev, M.F.M. Lutz, Phys. Lett. **B585**, (2004), 243

[29] M. Döring, E. Oset, D. Strottman, Phys. Lett. **B639**, (2006), 59